Available online at www.sciencedirect.com
ScienceDirect
J China Univ Mining & Technol 18 (2008) 0311–0315
JOURNAL OF CHINA UNIVERSITY OF MINING & TECHNOLOGY
www.elsevier.com/locate/jcumt

Numerical analysis of grinding power consumption of a vertical planetary mill

HAO Xue-di[1,2], ZHU Dong-mei[1], BIAN Zhi-rui[1], WANG Xin[2]

[1]*School of Mechanical Engineering, University of Science and Technology Beijing, Beijing 100083, China*
[2]*School of Mechanical Engineering, Hebei Polytechnic University, Tangshan, Hebei 063009, China*

Abstract: Planetary wheel rolling on a coal-bed was simplified as rigid wheel rolling on the coal-bed with a rigid base when a Vertical planetary mill (VPM) is running. Based on our analysis, we conclude that the Bekker formulation for computing rolling resistance is not applicable to calculate directly the rolling resistance of the wheel. According to the principle of the Bekker apparatus, pressure-sinkage curves were obtained by tests on a piece of mono-axial consolidation apparatus used in soil-mechanics. The deformation modulus of the coal-bed was calculated using elastic mechanics. A finite element model of the planetary wheel coal-bed was built up by the use of a rigid and a Drucker-Prager material model in LS-DYNA. According to the simulation results, the wheel rolling resistance, the grinding power consumption and the motor power of the mill were calculated and the mistake in the initial design of the mill was modified. The simulation results agree well with the results of the semi-industrial tests.
Key words: VPM; power-consumption; grinding; rolling; finite element method (FEM)

1 Introduction

The vertical planetary mill (VPM) is a novel, highly efficient, energy-conserving grinding mill with the advantages of requiring only a small amount of space, large capacity and low power consumption[1]. It has potentially wide applications in energy, metallurgy, chemical and construction industries, especially in grinding minerals with moderate or low hardness, such as coal. How to determine the grinding power consumption of any type of mill accurately is a very important issue in the design and use of the mill, given the promise of its greatest advantage, that of energy efficiency[2–3]. Unfortunately, due to the complexities of the issue itself, studies on the consumption of grinding mills are largely based on experiments. These experimental methods usually involve the following steps: manufacture the model of the machine, test the grinding performance, and calculate power consumption under conditions special in each case. The disadvantages of these methods include long periods, large expenditures and poor accuracy when conditions change.

Finite element methods (FEM) have been used in many engineering problems while they gradually improve. Especially, FEM is the main method adopted in solving many boundary problems that cannot be solved analytically. Our study focuses on the determination of power consumption of a mill using FEM on the basis of the parameters which characterize the deformation behavior of the ground materials, i.e., coal.

2 Structure and principle of VPM

The mill used for this study consists of an input cone, a bearing bracket, a shell, an attachment flange, a gearbox, a base, a discharge cone, a motor, and miscellaneous items (Fig. 1). The material to be ground enters into the grinding chamber from the input cone, and disperses along the interior cylindrical surface of the grinding chamber to form a material-bed under the gyroscopic effect, as shown in Fig. 2. The planetary wheel slides radially in the grooves of the planetary bracket also under the gyroscopic effect, rolls over and crushes the material. The ground material, after multi-pass grinding, is discharged by gravity through the discharge cone. In general, there are 3–8 planetary wheels per set, and 1–2 sets of wheels in VPM. For clarity, only one wheel in one set is illustrated in Fig. 2. We think that the motion of every wheel is similar according to the geometric and kinematical similarities. The following is the mechanical analysis of one wheel.

Received 03 November 2007; accepted 03 March 2008
Corresponding author. Tel: +86-15931900403; E-mail address: hxd2003@126.com

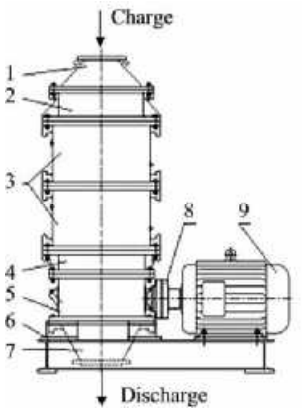

Fig. 1 The form of the VPM

1.Input cone; 2.Bearing bracket; 3.Shell; 4.Attachment flange; 5.Gear box; 6.Base; 7.Discharge cone; 8.Coupling; 9.Motor

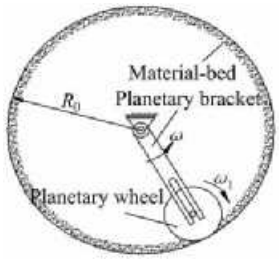

Fig. 2 Rolling state of the planetary wheel when VPM running

3 Mechanics of the rolling wheel

According to the principle of the mill as described above, the main power consumption of the mill is used for driving the planetary wheel rolling on the material, when the mill is running. To determine the rolling resistance of the wheel is very difficult, because it is related to many factors such as the characteristics of the ground material, the diameter of the planetary wheel and the rotational velocity of the main shaft. Some simplifications have to be made to model the planetary wheel material-bed system. In general, the following three assumptions are made:

1) the wheel rolling on the surface of the grinding chamber can be modeled as a wheel rolling on an infinite plane;

2) the tightly compacted ground material paved on the surface can be regarded as a continuum;

3) relative to that of the ground material, if the deformations of the wheel and the grinding chamber are very small, the wheel and the grinding chamber can be regarded as rigid bodies.

Based on these assumptions, the force diagram of the model of the wheel material-bed is illustrated in Fig. 3. The vertical load, W; the drag force, F_R and the interaction between the wheel and the ground material control the motion of the wheel. Since the shear stresses, τ, between the wheel and the ground material are much smaller than normal stresses, σ, we assume that only normal stresses are in effect between the wheel and the ground material. The maximum sinkage of the wheel is denoted as z_0. The rolling resistance of the wheel is numerically equal to the drag force, F_R, but symbolically inversed. The force can be analyzed by the resistance of a rigid wheel rolling on a soil-bed with a rigid base, using the principle of vehicle-terrain mechanics.

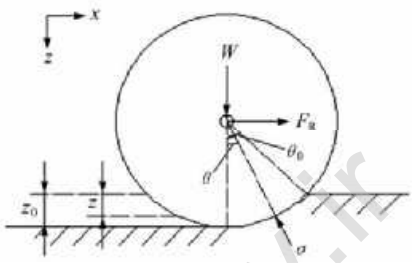

Fig. 3 Simplified mechanical model of the planetary wheel-material bed

Many investigators have studied the issue of the interaction between a rigid wheel and its terrain[4–7]. In general the pressure-sinkage k-model characterizing the deformation of the terrain is the most widely used[8], which represents the relationship between the pressure and the sinkage by a uniform equation:

$$p = kz^n \tag{1}$$

where p is the pressure exerted on the terrain, k the deformation modulus, related to the properties of the terrain, n the sinkage exponent of the terrain and z the vertical sinkage of the test plate.

Bekker modified the deformation modulus and proposed portioning k into the cohesion modulus k_c and the friction modulus k_φ. Then the relationship of the pressure and the sinkage can be written as[9]:

$$p = \left(\frac{k_c}{b} + k_\phi\right) z^n \tag{2}$$

According to Bekker's assumption, only the normal stresses between the rigid wheel and the terrain are in effect and the normal stresses are numerically equal to the pressure between the test plate and the terrain at the sinkage, z. It follows that:

$$\sigma r \sin\theta \mathrm{d}\theta = p\mathrm{d}z \tag{3}$$

$$\sigma r \cos\theta \mathrm{d}\theta = p\mathrm{d}x \tag{4}$$

where r is the radius of the wheel. Keeping force balance in the horizontal direction, as shown in Fig. 3, the drag force as well as the rolling resistance can be written as:

$$F_R = b\int_0^{\theta_0} \sigma r \sin\theta \mathrm{d}\theta \tag{5}$$

Similarly, for the force balance in the vertical direction, the vertical load, W, can be written as:

$$W = b\int_0^{\theta_0} \sigma r \cos\theta \mathrm{d}\theta \tag{6}$$

From Eqs.(2) to (6) the rolling resistance of the

rigid wheel can be written as:

$$F_{\mathrm{R}}=\frac{(3W)^{\frac{2n+2}{2n+1}}}{(3-n)^{\frac{2n+2}{2n+1}}(n+1)b^{\frac{1}{2n+1}}(\frac{k_{\mathrm{c}}}{b}+k_{\phi})^{\frac{1}{2n+1}}D^{\frac{n+1}{2n+1}}} \tag{7}$$

where D and b refer to the diameter and the width of the rigid wheel, respectively.

Experiments have shown that Eq.(7) is applicable to a rigid wheel rolling on most homogeneous terrains with moderate sinkage, except for clay. The larger the diameter of the wheel and the smaller the sinkage, the more accurate the computation. When the diameter is less than 500 mm, the smaller the diameter, the less accurate the calculation. Especially, when the slippage-rotation ratio is large, Eq.(7) can not be used. As well, given the derivation of Eq.(7) introduced above, the terrain is regarded as a semi-infinite body, but in fact, the material-bed is not thick enough, about 30 mm. Consequently, the parameters, k and n, of the deformation modulus of the material-bed are different from those of the terrain. If Eq.(7) is directly applied to the calculation of the rolling resistance of the planetary wheel, it will lead to an incorrect result. Calculations have shown that the rolling resistance, 4850 N, of the wheel using Eq.(7) and the power consumption, 382 kW, by the mill do not agree with experimental results. Eq.(7) needs to be modified for calculating the resistance of the wheel. Therefore, our study employs FEM to determine the rolling resistance of the wheel.

4 FEM of the rolling wheel

Some studies have analyzed the interaction of the rigid wheel and terrain utilizing FEM[10–11], which shows that a suitable material model is the key to simulate accurately the rolling of the rigid wheel. Given the principle of the Bekker apparatus, measuring the pressure-sinkage parameters, a mono-axial consolidation apparatus, used in soil mechanics tests and after some modifications, was used to determine the parameters characterizing the deformation of the ground coal-bed under compression (Fig. 4). The size of the coal particles in the sample ranged between 0–4 mm. Fig. 5 shows the curves of pressure-sinkage of the coal-bed from our experiments.

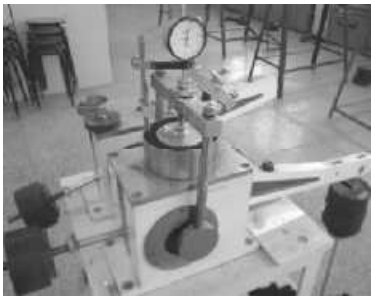

Fig. 4 Pressure-sinkage test apparatus of coal-bed

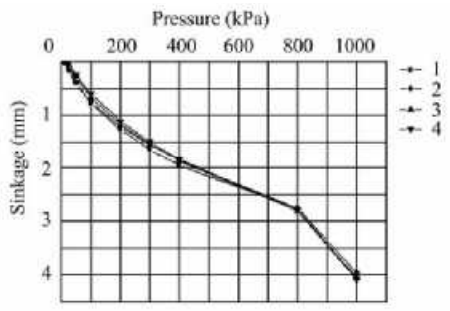

Fig. 5 Pressure-sinkage curves of coal bed (four groups of data)

From the data of Fig. 5, the modulus of compression, M, characterizing confined compression of the coal-bed can be obtained. Given the principle of theoretical elasticity, the unconfined compression modulus, E_0, of the coal-bed can be calculated[12], which is similar to Young's modulus, E. Since the irrecoverable plastic deformation must occur during compression of the coal-bed, an elastic-plastic constitutive model was adopted for the material of the coal-bed. The elastic-plastic constitutive equation can be written as[13]:

$$\{\mathrm{d}\sigma\}=\left[\boldsymbol{D}_{\mathrm{ep}}\right]\cdot\{\mathrm{d}\varepsilon\} \tag{8}$$

where $\{\mathrm{d}\sigma\}$ and $\{\mathrm{d}\varepsilon\}$ refer, respectively, to the stress and strain increments; $\left[\boldsymbol{D}_{\mathrm{ep}}\right]$ the elastic-plastic matrix, can be written as:

$$\left[\boldsymbol{D}_{\mathrm{ep}}\right]=[\boldsymbol{D}]-\frac{[\boldsymbol{D}]\left\{\frac{\partial g}{\partial\sigma}\right\}\left\{\frac{\partial f}{\partial\sigma}\right\}^{\mathrm{T}}[\boldsymbol{D}]}{\left\{\frac{\partial g}{\partial\sigma}\right\}^{\mathrm{T}}[\boldsymbol{D}]\left\{\frac{\partial f}{\partial\sigma}\right\}+A} \tag{9}$$

where g is the plastic potential, f the yield function, A the hardening function and $[\boldsymbol{D}]$ refers to the elastic matrix.

Due to the kinetic characteristics of the issue, the explicit FEM code, LS-DYNA, was utilized. LS-DYNA is an excellent explicit FEM software, which has been adopted to solve many complex problems. Xia, et al selected the Johnson-Cook plasticity material model for investigating deformations of cobalt-rich crusts[14]. The Drucker-Prager material model provided by LS-DYNA is suitable to simulate the deformation of coal-beds. Therefore, we have opted for this material model. Based on the tests above, the elastic and plastic parameters of the material model were calculated. The results are shown in Table 1.

Table 1 Parameters of the coal-bed

Parameters	Values
Density ρ (kg/m^3)	1500
Shear modulus G (MPa)	3.245
Poisson's ratio μ	0.2
Internal friction angle (°)	32
Dilation angle (°)	0

The FEM model of the wheel and the coal-bed was initially built utilizing ANSYS. Due to symmetry of the issue, a half geometry of the wheel is modeled to reduce the size of the model (Fig. 6). The degrees of freedom in the vertical and the rolling directions of the nodes in the bottom of the coal-bed are removed, due to the coal-bed lying on the rigid surface of the grinding chamber. The vertical boundary of the coal-bed in the rolling direction was set to a non-reflecting boundary condition in order to eliminate from the results the contamination of reflecting waves.

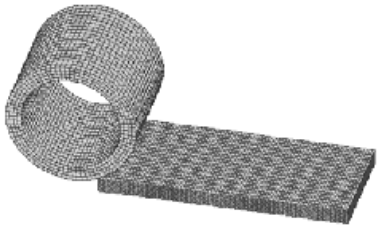

Fig. 6 FEM model of the planetary wheel-coal bed

According to practical operating conditions, the coal-bed is 30 mm in thickness, the radius of the roller is 130 mm, the maximum sinkage 10 mm, the translational velocity of the wheel 1 m/s and simulation time 0.5 s. When the initialization of the model is finished, a key file for LS-DYNA running is generated by ANSYS. Because ANSYS does not support many kinds of material models in LS-DYNA, the generated key file had to be modified to involve the Drucker-Prager material model. After this modification, the key file was ready for LS-DYNA running. The simulation results are shown in Figs. 7–9.

5 Results and discussion

The interface pressure contours between the roller and the coal-bed are shown in Fig. 7. Fig. 7a is the state at 0.16 s, and Fig. 7b is the state at 0.3 s. Comparing the two figures, it shows that the length of the interface between the wheel and the coal-bed at 0.3 s is longer than that at 0.16 s. Rebounding of the coal-bed after the rolling wheel passed over the coal-bed is the cause of this result, which was also reported by Chiroux, et al[11]. More efforts are need to eliminate this effect. The bow in the top of the coal-bed, ahead of the wheel, shows that the wheel pushes the coal particles forward and upward when rolling, which agrees with the results from other reported tests.

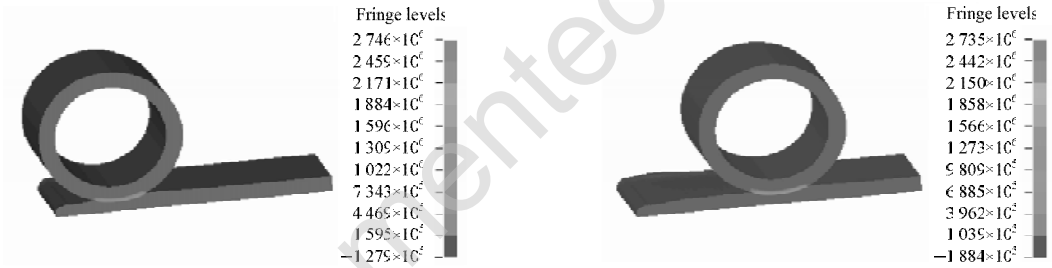

(a) State at 0.16 s (b) State at 0.3 s

Fig. 7 Interface pressure contours with rolling planetary wheel

The normal curves and the shear stresses via the angle θ, as shown in Fig. 3, are shown in Fig. 8. The normal stresses have a single-peaked distribution; the two sides of the peak point are not symmetric. The maximum value for the normal stresses is not at the lowest point under the centerline of the wheel, but at an angle of 0.36° ahead of the lowest point of the wheel, as shown in Fig. 8. There are two maximum shear stresses, which are approximate 1/5–1/6 of the normal stresses. Sequentially, it is reasonable to ignore the contribution of the shear stresses to the rolling resistance of the wheel during the application of Eq.(7).

The curves of the rolling resistance over time are shown in Fig. 9. During the start-up process the force grows to a maximum and then gradually declines. Between 0.2–0.4 s the force fluctuates around a stable value. After 0.4 s, the force gradually declines to zero when the wheel rolls over the coal-bed. The maximum force is related to the kinetic effects of loading, caused initially by the wheel knocking on the coal-bed. The fluctuation of the force during 0.2–0.4 s is

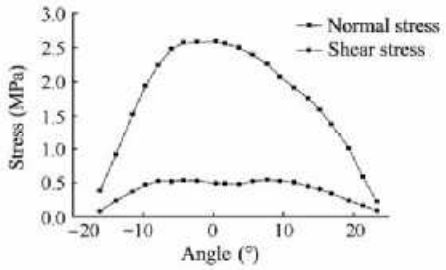

Fig. 8 Curves of interface stresses

related to the mesh size and the translational velocity of the wheel, which can be reduced by slowing down the translational velocity or by refining the mesh of the model. But the value of the translational velocity is set according to the operating conditions of the mill, which can not change very much under practical conditions. As well, refining the mesh of the model will greatly increase computational time. So a reasonable translational velocity and a computationally eco-

nomic refinement of the mesh were adopted in our study. Based on the data of five-poit averaged calculation to the simulation points, a stable average value of the force was obtained, 1143 N, as shown in Fig. 9.

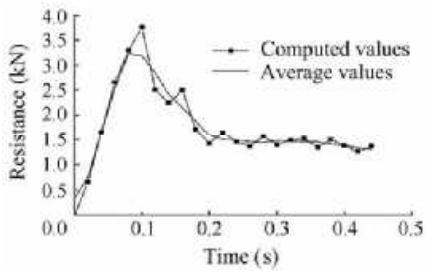

Fig. 9 Curves of rolling resistance-time of planetary wheel

The real value of the force is twice that of the average value due to the symmetry of the model. The motion of the wheel is regarded as a non-radial translation when the mill is stably running, as shown in Fig. 2; as a sequence, the rotational radius of the wheel is constant. The grinding power consumption of the mill equals the product of the stable resistance of the wheel and the translational velocity of the wheel centroid. The translational velocity of the wheel centroid can be written as:

$$v = R\omega \tag{10}$$

Then, the grinding power consumption of the mill can be written as:

$$P_0 = 2iF_R v = 2iF_R R\omega \tag{11}$$

where P_0 is the grinding power consumption of the mill, i the number of the wheel, R the rotational radius of the wheel, which equals $R_0 - r$ (Fig. 2), ω is the rotational velocity of the main shaft.

For the mill of Type LXM1200, i is 8, R is 0.47 m, ω is 20.94 rad/s. The grinding power consumption of the mill is 227 kW, calculated from Eq.(11) when the mill is running under stable conditions. A motor with 110 kW standard power was used for the mill in its initial design. In semi-industrial tests, however, the mill stopped for lack of power when approaching the specification load gradually. The simulation results above can suggest the reason clearly. Based on the computed value of the grinding power consumption of the mill, accounting for the loss of the drive system and the power for reservation, the standard power of the motor for the mill should be 260 kW. Semi-industrial tests have shown that a shortage of power of mills driven by a new motor do no longer occur when mills are running under a specified load.

6 Conclusions

1) The Bekker formulation for calculating the rolling resistance of a rigid wheel is not directly applicable to the computation of resistance of a planetary wheel. More efforts are needed to make it applicable for calculating this force.

2) Employment of FEM to analyze the rolling resistance of a planetary wheel was successful, which can provide a relatively accurate estimate of the force.

3) At our study at hand, the number of the planetary wheel is 8, the rotational radius of the wheel is 0.47 m, the rotational velocity of the main shaft is 20.94 rad/s, the averaged grinding power consumption of VPM is 227 kW.

Acknowledgements

We gratefully acknowledge the help from the Yankuang Lunan Fertilizer Plant for providing support for the semi-industrial tests.

References

[1] Hao X D, Bian Z R, Liu L, et al. 3-D numerical simulation of the flow field in the chamber of the vertical planetary mill. *Metallurgical Equipment*, 2004, 158(4): 14–17. (In Chinese)

[2] Sun C B, Li R H, Lu S C, et al. Operating principle and characteristic of the Szego Mill. *Mining & Processing Equipment*, 1998(7): 18–20. (In Chinese)

[3] Li R T, Peng L Z, Xie L. Dynamics analysis of vertical planetary pulverizing system. *Metal Mine*, 2000, 291(9): 37–38. (In Chinese)

[4] Wanjii S, Hiroma T, Ota Y, et al. Prediction of wheel performance by analysis of normal and tangential stress distributions under the wheel-soil interface. *Journal of Terramechanics*, 1997, 34(3): 165–186.

[5] Shmuleich I, Mussel U, Wolf D. The effect of velocity on rigid wheel performance. *Journal of Terramechanics*, 1998(35): 189–207.

[6] Shibly H, Iagnemma K, Dubowsky S. An equivalent soil mechanics formulation for rigid wheels in deformable terrain with application to planetary exploration rovers. *Journal of Terramechanics*, 2005(4): 1–13.

[7] Fukami K, Masami U, Hashiguchi K, et al. Mathematical models for soil displacement under a rigid wheel. *Journal of Terramechanics*, 2006(43): 287–301.

[8] Wang J L. *Research of Modeling and Simulation on Interaction Between Elastic Tire and Terrain* [Master dissertation]. Changchun: Jilin University, 2002. (In Chinese)

[9] Zhang K J. *Vehicle-Terramechanics*. Beijing: National Defense Industry Press, 2002. (In Chinese)

[10] Raper R L, Johson C E, Beiley A C, et al. Prediction of soil stresses beneath a rigid wheel. *J Agic Eng Res*, 1995(61): 57–62.

[11] Chiroux R C, Foster W A, Johson C E, et al. Three-dimensional finite element analysis of soil interaction with a rigid wheel. *Applied Mechanics and Computation*, 2005(162): 707–222.

[12] Zhang X Y, Yan S W. *Fundamentals of Geotechnics Plasticity*. Tianjin: Tianjin University Press, 2004. (In Chinese)

[13] Niu Z R, Yang G T. Studies on the displacement of soils subjected to impact loading. *Rock and Soil Mechanics*, 2005, 26(11): 1743–1748. (In Chinese)

[14] Xia Y M, Ma Z G, Bu Y Y, et al. Simulation of cobalt-rich crust's crushing process based on ANSYS. *Journal of China University of Mining & Technology*, 2006, 16(1): 28–32.